

# Theory and Applications of Optical Gyroscopes: Part II

The operating principles and the functions of fiber-optic gyroscopes, including open- and closed-loop interferometric devices and resonant fiber-optic gyros, are investigated.

**P**art I of this article, which appeared in the July issue of *Sensors*, examined the operating principles and functions of active and passive ring laser gyros. Part II takes up fiber-optic gyroscopes. The figures, equations, and references in Part II are numbered consecutively to those in Part I.

## OPEN-LOOP INTERFEROMETRIC FIBER-OPTIC GYROS

The concurrent development of optical fiber technology, spurred mainly by the communications industry, presented a potential low-cost alternative to the high-tolerance machining and clean-room assembly required for ring laser gyros. The glass fiber in essence forms an internally reflective waveguide for optical energy, along the lines of a small-diameter linear implementation of the doughnut-shaped mirror cavity conceptualized by Schulz-DuBois [4]. The use of multiple turns of fiber means the resultant path-length change due to the Sagnac effect is essentially multiplied by a factor  $N$  equal to the integer number of turns, thereby providing significantly improved resolution [12]. An additional advantage of the fiber-optic configuration stems from the fact that operation is not dependent on a high-finesse cavity, thereby significantly reducing manu-

facturing costs [20].

The *refractive index*  $n$  relates the speed of light in a particular medium to the speed of light in a vacuum:

$$n = \frac{c}{c_m} \quad (4)$$

where:

- $n$  = refractive index of medium
- $c$  = speed of light in a vacuum
- $c_m$  = speed of light in medium

*Step-index multimode fiber* (see Figure 5) is made up of a core region of glass with index of refraction  $n_{co}$ , surrounded by a protective cladding with a lower index of refraction  $n_{cl}$  [21]. The lower refractive index in the cladding is necessary to ensure total internal reflection of the light propagating through the core region. Step-index refers to this "stepped" discontinuity in the refractive index that occurs at the interface of the core and cladding.

As shown in Figure 6 (page 28), as long as the entry angle (with respect to the waveguide axis) of an incoming ray is less than a certain critical angle  $\theta_c$ , the ray will be guided down the fiber, virtually without loss. The *numerical aperture* of the fiber quantifies this parameter of acceptance (i.e., the light-collecting ability of the fiber), and is defined as [21]:

$$NA = \sin \theta_c = \sqrt{n_{co}^2 - n_{cl}^2} \quad (5)$$

where:

- $NA$  = numerical aperture of the fiber
- $\theta_c$  = critical angle of acceptance
- $n_{co}$  = index of refraction of glass core
- $n_{cl}$  = index of refraction of cladding

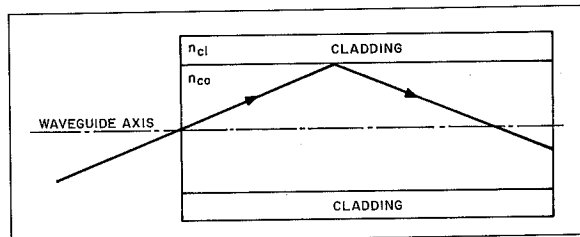


Figure 5. The distinctive "step" discontinuity in the refractive index at the interface between the core and the cladding gives rise to the terminology "step-index" fiber. (Adapted from [21].)

As shown in Figure 6, a number of rays following paths of different lengths can simultaneously propagate down the fiber, as long as their respective entry angles are less than the critical angle of acceptance  $\theta_c$ . Multiple-path propagation of this nature occurs when the core diameter is much larger than the wavelength of the guided energy, giving rise to the term multimode fiber. Such multimode operation is clearly undesirable in gyro applications, where the objective is to eliminate all nonreciprocal conditions other than that imposed by the Sagnac effect itself. As the diameter of the core is reduced to approach the operating wavelength, a cutoff condition is reached where just a single mode is allowed to propagate, constrained to travel only along the waveguide axis [21].

Light can randomly change polarization states as it propagates through standard *single-mode fiber*. The use of special *polarization-maintaining fiber*, such as PRSM Corning, maintains the original polarization state of the light along the path of travel [3]. This is important, because light of different polarization states travels through an optical fiber at different speeds. Figure 7 (page 28)

H.R. Everett, Naval Command Control and Ocean Surveillance Center

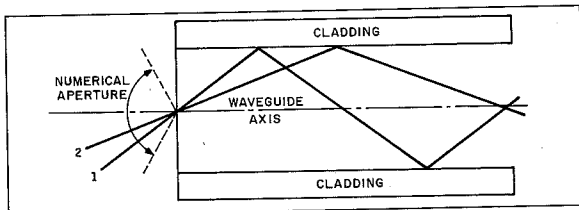


Figure 6. Entry angles of incoming rays 1 and 2 determine the propagation paths in the fiber core. (Adapted from [21].)

shows the typical "minimum-reciprocal" IFOG configuration. Polarization-maintaining single-mode fiber [21] is used to ensure that the two counterpropagating beams in the loop follow identical paths in the absence of rotation.

The Sagnac phase shift between the two beams introduced by gyro rotation is given by [12]:

$$Z_R = \frac{LD}{\lambda c} \Omega \quad (6)$$

where:

$Z_R$  = number of fringes of phase shift due to gyro rotation

$L$  = length of fiber cable in loop

$D$  = diameter of loop

$\lambda$  = wavelength of optical energy

$c$  = speed of light in a vacuum

$\Omega$  = rotation rate

The stability of the scale factor relating  $Z_R$  to  $\Omega$  in Equation 6 is thus dependent on the stability of  $L$ ,  $D$ , and  $\lambda$  [11]. Practical implementations usually operate over plus or minus half a fringe (i.e.,  $\pm \pi$  radian of phase difference)

with a theoretical sensitivity of  $10^{-6}$  radian or less of phase shift [22]. IFOG sensitivity may be improved by increasing  $L$  (i.e., adding more turns of fiber in the sensing loop), peaking at an optimal length on the order of several kilometers, after which the fiber attenuation (1 dB

per kilometer typical) begins to degrade performance [11]. This large amount of required fiber represents a rather significant percentage of overall system cost.

The two counterpropagating beams reunite at the detector, which monitors the cosinusoidal intensity changes caused by constructive and destructive interference. The peak intensity occurs as shown in Figure 8 (page 29) at the point of zero rotation rate, where the phase shift  $\Delta\phi$  between the counterpropagating beams is equal to zero. Unfortunately, there is no way to determine the direction of rotation directly from the intensity information (as can be

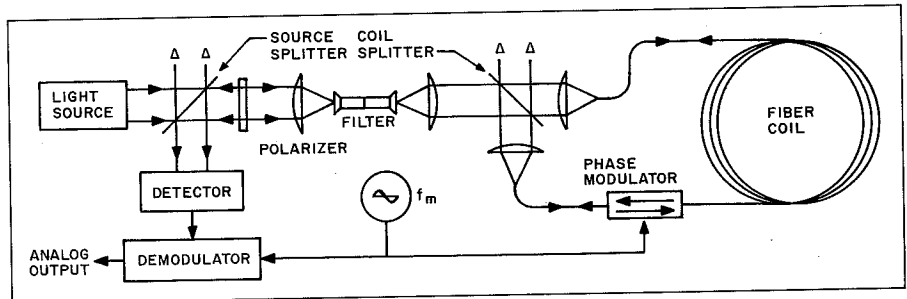


Figure 7. The popular "minimum-reciprocal" IFOG configuration uses a low-coherence light source (such as a superluminescent diode) in conjunction with a multiturn loop of polarization-maintaining single-mode fiber to yield a nonlinear analog output signal. (Adapted from [11,24].)

This **PREVIEW** is intended for audiences in product design, R&D, predictive & preventive maintenance and process control who want to make their jobs easier, less time consuming and more cost efficient using infrared imaging.

**RATED IR**

**FSI** FLIR SYSTEMS™ Get this exciting **FREE VIDEO** to see in graphic detail how infrared imaging can help you do your job better and faster. Just call the leader in infrared imaging systems — FLIR Systems — today at **1-800-322-3731**.

16505 SW 72nd Ave., Portland, OR 97224, (503)684-3731, Fax (503)684-3207

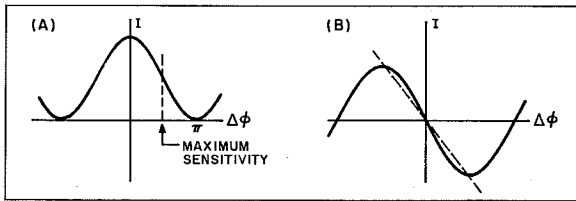


Figure 8. A nonreciprocal phase shift is introduced in the open-loop IFOG to shift operation to the region of maximum sensitivity shown in the plot of detector intensity vs. phase shift (A), resulting in the unambiguous demodulator output shown in (B). (Adapted from [11].)

inferred from the symmetrical nature of the plot with respect to the Y-axis), and the sensitivity of  $I$  to small changes in rotation rate is greatly reduced due to the horizontal nature of the slope [20].

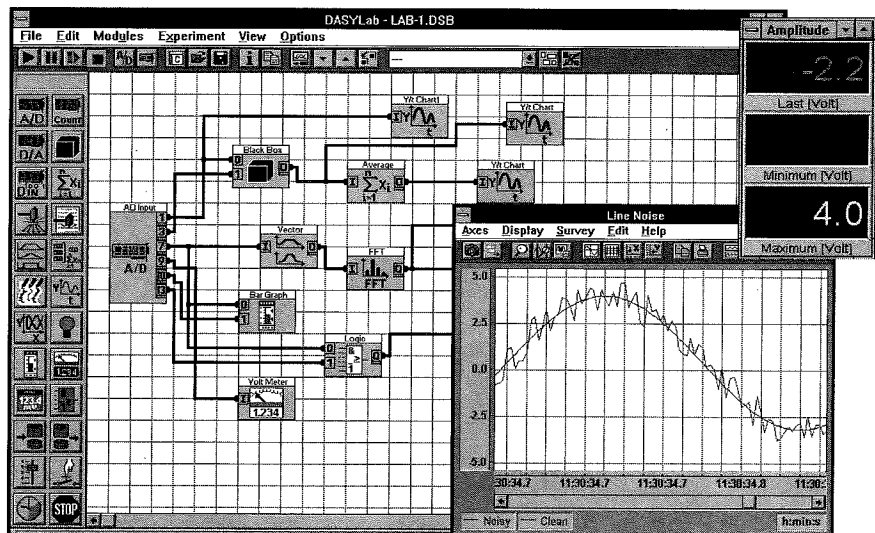
To overcome these deficiencies, nonreciprocal phase shifts between the two beams are introduced at an oscillatory rate  $\omega$ , usually by phase modulation of the beams near one end of the interferometer coil [10]. This phase modulation can be accomplished using a length of fiber wound around a piezoelectric cylinder, and introduces a bias of  $\pi/2$  to shift the operating point over into the region of maximum sensitivity on the response curve as shown in Figure 8A [11]. (The output of the photodetector is then synchronously demodulated and filtered to yield the sinusoidal analog representation of  $\Delta\phi$  shown in Figure 8B. Note that the direction of rotation is now easily determined from the sign of the output. Disadvantages of this open-loop approach include the nonlinear relationship of the demodulated output to rotation rate  $\Omega$ , and the inherent susceptibility to errors caused by variations in the light source intensity or component tolerances. As Blake [20] points out, it is difficult to achieve good linearity in analog electronic componentry over six orders of magnitude of dynamic range.

An interesting characteristic of the open-loop IFOG is the absence of any narrow-band laser source [23], the enabling technology allowing the Sagnac effect to reach practical implementation in the first place. A low-coherence source, such as a superluminescent diode (SLD), is typically used instead to reduce the effects of noise [12,24], the primary source of which is backscattering within the fiber and at any interfaces. As a result of such backscatter, in addition to the two primary counter-propagating waves in the loop there are a number of parasitic waves that yield

secondary interferometers [22]. The limited temporal coherence of the broadband SLD causes any interference due to backscattering to average to zero, suppressing the contrast of these spurious interferometers. The detection system becomes sensitive only to the interference between waves that followed identical paths [11,22].

The open-loop IFOG is attractive from the standpoint of reduced manufacturing costs; high tolerance to shock and vibration; insensitivity to gravitational effects; quick startup; and fairly good sensitivity in terms of bias drift rate and the random walk coefficient. Coil geometry is not critical, and no path-length control is needed. Disadvantages include the long length of optical fiber required (relative to other fiber-optic gyro designs, as discussed later); limited dynamic range in comparison to active ring laser

# DASYLab™



## Chock-full of goodies!

DASYLab is more than just the premier Windows-based data acquisition and control program. It's chock-full of little touches that make your job easier. For instance, note the slide bar on the strip chart. You can scroll the chart backwards to see data that has already passed through the window, even while acquiring more data!

You can stream data to disk at speeds in excess of 200KHz, and display samples of the data to make a visual check on the data during acquisition.

And there's lots more, too. Flexibility in setting up displays, including grouping of instruments. Automatic or manual changes to the displays while acquiring data. Operator messages. Event handling. Real-time data analysis. A programmable waveform generator. IEEE, RS-232, DDE support. The list goes on...

For more information and a demo disk contact:

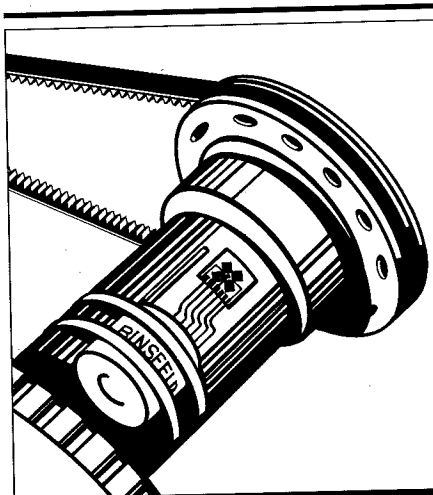
You can use DASYLab with data acquisition hardware from:

- ADAC, Advantech, Analog Devices,
- Analogic, Computer Boards, Contec,
- Data Electronics, Data Translation,
- Gage Applied Sciences,
- Intelligent Instrumentation,
- Innovative Integration, Iotech,
- Keithley, Measurement Systems,
- Microstar Laboratories,
- National Instruments,
- United Electronics Industries

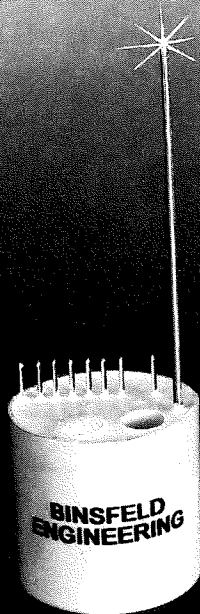
DASYLab and DASYTEC are trademarks of Datalog GmbH  
Windows is a trademark of Microsoft Corporation

DASYTEC®

P.O. Box 748 • 14 Boston Post Road  
Amherst, NH 03031  
Tel. (603) 672-7061 • FAX (603) 673-7892  
73211,3360@compuserve.com



**SENSORS IN  
MOTION  
DIFFICULT TO WIRE?  
BINSFELD  
TELEMETRY  
MAKES  
THE CONNECTION**



**SINGLE CHANNEL SYSTEMS  
under \$3000**

**Transmits torque • temperature •  
acceleration • pressure • voltage**  
**BINSFELD ENGINEERING**

*binsfeld*

4571 West MacFarlane, Maple City, MI 49664  
800-524-3327

gyros; and scale factor variations due to analog component drifts [25]. Open-loop configurations are therefore most suited to the needs of low-cost systems in applications requiring only moderate accuracy, such as gyrocompassing in automobile navigation, pitch and roll indicators, and attitude stabilization.

### CLOSED-LOOP INTERFEROMETRIC FIBER-OPTIC GYROS

For applications (such as aircraft navigation) demanding higher accuracy than that afforded by the open-loop IFOG, the closed-loop configuration offers significant promise, with drifts in the 0.001–0.01°/hr range and scale factor stabilities > 100 ppm [25]. Closed-loop digital signal processing is considerably more complex than the analog signal processing employed on open-loop IFOG configurations. Feedback into a frequency- or phase-shifting element (see Figure 9) is used to cancel the rotationally induced Sagnac phase shift. Because the system is always operated at a null condition where  $\Delta\phi$  is equal to zero, minor variations in light-source intensity and analog component tolerances have a markedly reduced effect [11].

Referring again to Figure 9, the output of the *demodulator* is passed to a servo amplifier that in turn drives a *non-reciprocal phase transducer* (NRPT), typically an electro-optic frequency shifter placed within the fiber interferometer [11]. The NRPT introduces a frequency difference between the two counterpropagating beams, resulting in an associated fringe shift at the detector given by [10]:

$$Z_F = - \frac{\Delta f L n}{c} \quad (7)$$

where:

- $Z_F$  = fringe shift due to frequency difference
- $\Delta f$  = frequency difference introduced by the NRPT
- $L$  = length of fiber cable in loop
- $n$  = index of refraction
- $c$  = speed of light

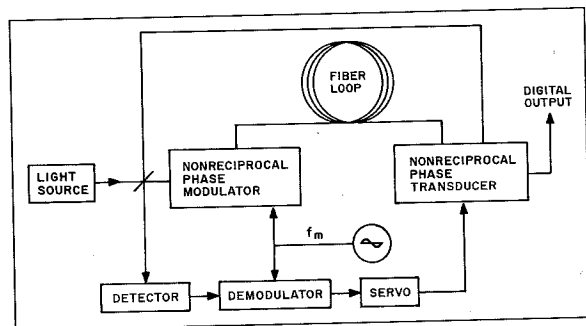


Figure 9. The closed-loop IFOG uses a nonreciprocal phase transducer to null out the Sagnac phase shift  $\Delta\theta$  introduced by rotation rate  $\Omega$ . (Adapted from [11].)

To null out  $\Delta\phi$  at the detector, the fringe shift  $Z_R$  due to gyro rotation must be precisely offset by the fringe shift  $Z_F$  due to the relative frequency difference of the two beams:

$$\Delta\phi = Z_R + Z_F = 0 \quad (8)$$

Substituting the previous expressions for  $Z_F$  and  $Z_R$  and solving for  $\Delta f$  yields [10,11]:

$$\Delta f = \frac{4AN}{n\lambda L} \Omega = \frac{4A}{n\lambda P} \Omega = \frac{D}{n\lambda} \Omega \quad (9)$$

where:

- $A$  = area of fiber loop
- $N$  = number of turns in loop
- $L$  = length of fiber cable in loop
- $P$  = loop perimeter
- $D$  = loop diameter

The gyro output, being the servo-controlled frequency shift  $\Delta f$  imparted by the NRPT, is thus inherently digital, as opposed to an analog DC voltage level, and also linear.

Ezekiel and Arditty [11] list the following advantages of the closed-loop configuration over the open-loop IFOG design previously discussed:

- It is independent of intensity variations in the light source, since the system is operated at null.
- It is independent of individual component gains (assuming high open-loop gain maintained).
- Linearity and stability depend only on the non-reciprocal phase transducer.

### RESONANT FIBER-OPTIC GYROS

The *resonant fiber-optic gyro* (RFOG) evolved as a solid-state derivative of the passive ring resonator gyro. A passive

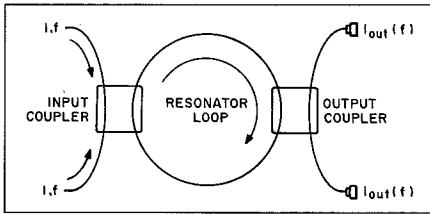


Figure 10. In the resonant fiber-optic gyro (RFOG), maximum optical coupling into the loop occurs at the resonant frequency that yields an integral number of wavelengths corresponding to the loop perimeter. (Adapted from [19].)

resonant cavity is formed from a multi-turn closed loop of optical fiber as shown in Figure 10. An input coupler provides a means for injecting frequency-modulated light from a laser source into the resonant loop in both the clockwise and counterclockwise directions. As the frequency of the modulated light passes through a value such that the perimeter of the loop precisely matches an integral number of wavelengths at that frequency, input energy is strongly coupled into the loop [19]. In the absence of loop rotation, maximum coupling for both beam directions occurs in a sharp peak centered at this resonant frequency.

If the loop is caused to rotate in the clockwise direction, of course, the Sagnac effect causes the perceived loop perimeter to lengthen for the clockwise-traveling beam, and to shorten for the counterclockwise-traveling beam. The resonant frequencies must shift accordingly, and energy is consequently coupled into the loop at two different frequencies and directions during each cycle of the sinusoidal FM sweep. An output coupler samples the intensity of the energy in the loop by passing a percentage of the two counter-rotating beams to their respective detectors, as

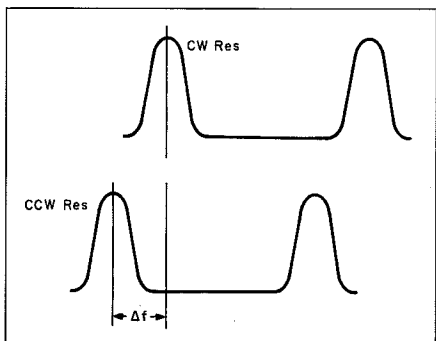


Figure 11. The difference ( $\Delta f$ ) between the resonance frequencies associated with the clockwise and counterclockwise beams provides a measure of rotation rate  $\Omega$ . (Adapted from [19].)

## THERMOELECTRIC COOLING FROM MELCOR



For maximum cooling in minimum space, nothing rivals Frigichip® thermoelectric (Peltier effect) coolers from MELCOR. For three decades, these miniaturized solid state heat pumps have provided precision cooling to temperatures far below ambient with extremely low space and current requirements. Choose from more than 150 standard single-stage coolers...from subminiature, low

capacity to compact, high capacity modules. Plus standard and custom-designed multistage cascades. Frigichips are ideal for a wide range of applications, including electronic instrumentation, communications and military systems, electro-optics, medical and laboratory apparatus, consumer appliances and a lot more. Call our applications group today!

**MELCOR**

Melcor Corporation

1040 Spruce Street • Trenton, NJ 08648  
609/393-4178 Fax: 609/393-9461

## ... "mini" mize size, maximize performance



Sensors shown actual size

## New ICP® MINIATURE ACCELEROMETERS AND PRESSURE MICROSENSOR

The perfect solution for dynamic pressure, shock and vibration measurements!

■ Printed Circuit Boards ■ Small Components ■ Sheet Metal Panels ■ Vibration Stress Screening ■ Non Contact Shock Measurements ■ Disk Drive Mechanisms ■ Modal Analysis ■ MIL-STD-810E Testing ■ Projectile Velocity

PCB offers a wide variety of miniature accelerometers with built-in electronics in single or triaxial configurations.

For more information, contact an applications engineer at:

**PCB Piezotronics, Inc.**

3425 Walden Ave., Depew NY 14043  
716-684-0001, Fax 716-684-0987, Twx 710-263-1371



®ICP is a registered trademark of PCB Piezotronics, Inc.

shown in Figure 10.

The demodulated output from these detectors will show resonance peaks as illustrated in Figure 11 (page 31) separated by a frequency difference  $\Delta f$  given by the following [19]:

$$\Delta f = \frac{D}{\lambda n} \Omega \quad (10)$$

where:

- $\Delta f$  = frequency difference between counterpropagating beams
- $D$  = diameter of resonant loop

- $\lambda$  = free-space wavelength of laser
- $n$  = refractive index of fiber

In practice, the laser frequency is usually adjusted to maintain resonance in one direction, while an electro-optical frequency shifter is used to drive the other direction back into resonance. This requires a frequency shift of  $2 \times$  the induced Sagnac effect, since the first direction has been locked. Actual rotation rate is then determined from the magnitude of the frequency shift.

Like the IFOG, the all-solid-state RFOG is attractive from the standpoint of high reliability, long life, quick startup, and light weight. The principal advantage of the RFOG, however, is that it requires significantly less fiber (10–100  $\times$  less) in the sensing coil than the IFOG configuration, while achieving the same shot-noise-limited performance [19]. Sanders attributes this to the fact that light traverses the sensing loop multiple times, as opposed to once in the IFOG counterpart. On the downside are the requirements for a highly coherent source and extremely low-loss fiber components [25].

## REFERENCES

2. G.J. Martin. Feb 1986. "Gyroscopes May Cease Spinning," *IEEE Spectrum*:48-53.
3. M.K. Reunert. Aug 1993. "Fiber-Optic Gyroscopes: Principles and Applications," *Sensors*:37-38.
4. E.O. Schulz-DuBois. Aug 1966. "Alternative Interpretation of Rotation Rate Sensing by Ring Laser," *IEEE J Quantum Electronics*, Vol. QE-2, No. 8:299-305.
10. E. Udd. 1991. "Fiber Optic Sensors Based on the Sagnac Interferometer and Passive Ring Resonator," *Fiber Optic Sensors: An Introduction for Engineers and Scientists*, E. Udd, ed., John Wiley, New York:233-269.
11. S. Ezekiel and H.J. Arditi, eds. 1982. "Fiber Optic Rotation Sensors and Related Technologies," *Proc First International Conference*, MIT, Springer-Verlag, New York.
12. E. Udd. Dec 1985. "Fiber-optic vs. Ring Laser Gyros: An Assessment of the Technology," *Laser Focus/Electro Optics*.
19. G.A. Sanders. Sept 1992. "Critical Review of Resonator Fiber Optic Gyroscopes Technology," *Fiber Optic Sensors*, E. Udd, ed., Vol. CR44, SPIE Optical Engineering Press, Bellingham, WA.
20. J. Blake et al. Oct 1989. "Design, Development, and Test of a 3-Inch Open Loop All Fiber Gyro," *MSD-TR-89-21*, 14th Biennial Guidance Test Symposium, Holloman AFB, NM:255-266.
21. D.A. Nolan et al. 1991. "Optical Fibers," *Fiber Optic Sensors: An Introduction for Engineers and Scientists*, E. Udd, ed., John Wiley, New York:9-26.
22. H.C. Lefevre. Sept 1992. "The Interferometric Fiber-Optic Gyroscopes," *Fiber Optic Sensors*, E. Udd, ed., Vol. CR44, SPIE Optical Engineering Press, Bellingham, WA.
23. W.K. Burns et al. 1983. "Fiber-Optic Gyroscopes with Broad-Band Sources," *IEEE J Lightwave Technology*, Vol. LT-1:98.
24. S. Tai et al. 1986. "All-Fiber Gyroscopes Using Depolarized Superluminescent Diode," *Electronic Letters*, Vol. 22:546.
25. P. Adrian. Sept 1991. "Technical Advances in Fiber-Optic Sensors: Theory and Applications," *Sensors*:23-45.

*Adapted from H.R. Everett, Sensors for Mobile Robots: Theory and Application. Ch. 13, "Gyroscopes." AK Peters Ltd, Wellesley, MA, 617-235-2210. ISBN 1-56881-048-2; 550 pp. \$59.95. Reviewed in Sensors, June 1995, p. 59.*

H.R. Everett is MDARS Technical Director, Naval Command Control and Ocean Surveillance Center, San Diego, CA 92152-5000; 619-553-3672, fax 619-553-6188.

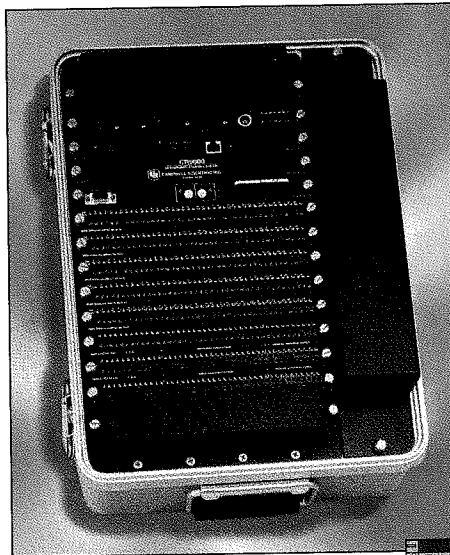
## Reader Feedback

To rate this article, circle the appropriate number on the Reader Service Card.

4	14	24
Excellent	Good	Fair

# Rugged and Fast

## CR9000 Measurement and Control System for Acceleration and Vibration Testing



### Hardware

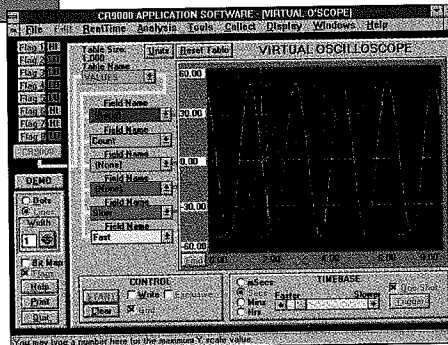
- 32-bit transputer with FPU
- 16-bit, 100 kHz A/D
- Up to 126 differential measurements
- 50 mV to 50 V input ranges
- Programmable analog outputs
- Digital inputs/outputs
- PCMCIA type I, II, III support
- Fiber optic, RS422, RS232
- Portable—up to 14 hours on a full charge
- Time or event power on/off
- Operation in harsh environments

### Software

- Simple program generation
- Wiring diagram creation
- Real-time and historical graphing
- Virtual instrument display

### Measurements

- Thermocouples—type T, E, K, J, B, R, and S
- Accelerometers and microphones
- Thermistors and PRTs
- Pressure, force, and strain sensors
- Pulse and frequency sensors



**Includes fully integrated Windows software**

**Campbell Reliability**

**CAMPBELL SCIENTIFIC, INC.**  
815 W. 1800 N. • Logan, Utah 84321-1784 • (801) 753-2342 • FAX (801) 750-9540